Proceedings of the 2003 IEEE
International Conference on Robotics & Automation
Taipei, Taiwan, September 14-19, 2003

A New Active Microendoscope for Exploring the Sub-arachnoid Space in the Spinal Cord

Luca Ascari[1] and Cesare Stefanini[1] and Arianna Menciassi[1] and Sambit Sahoo[2]
and Pierre Rabischong[3] and Paolo Dario[1]
1. CRIM - Scuola Superiore Sant'Anna, Pisa, Italy
Luca Ascari E-mail: ascari@sssup.it
2. SMST, IIT, Kharagpur, West Bengal, India
3. Laboratory of Anatomy, Faculté de Médécine de Montpellier, France

***Abstract*— This paper presents the design, development and preliminary test of a new active microendoscope for neuroendoscopy and therapy of the spinal cord. Endoscopy of the spinal sub-arachnoid space is useful for some pathologies, but it is a very challenging task for several reasons: the navigation space is very narrow, there are many blood vessels and delicate structures which could be damaged by manoeuvres and large forces and, finally, the Cerebro-Spinal Fluid (CSF) is a peculiar environment which must be preserved. An innovative method for active safe navigation in the sub-arachnoid space has been devised, based on hydrojets sustentation of the endoscope. The hydrojets, if appropriately tuned and oriented, allow the tip of the endoscope to avoid the delicate structures of the spinal cord and could also assist propulsion. A MATLAB simulation of the hydrojets is illustrated and a digital controller for the regulation of the hydrojets is demonstrated. The pressure ripple is about 5%, as tested experimentally on a 2D simulator. A prototype of steerable microendoscope whose tip is equipped with hydrojets has been fabricated and tested in an artificial path simulating the sub-arachnoid space. Performance are quite interesting.**

I. Introduction

There are many different pathological diseases affecting the spinal cord. In addition to traumas, which represent the major part, there are aneurysms, tumours, infections, degenerative processes and late surgical complications [1].

Medical imaging is a non invasive diagnostic technique very often exploited. On the other hand, the resolution of the images, with or without contrast media, is still not comparable with the direct vision of the anatomical structures [2]. Often MRI or CT images are not able to provide sufficient useful information for diagnoses [3]. Concerning interventions, traditional open surgery procedures have major drawbacks in case of traumatic lesions of the spinal cord. In fact these procedures, which always cause important reactions *in situ*, only allow restoration of the mechanical functions and decompression of the spinal cord. It is quite impossible to intervene on the lesion itself, mainly because of the difficulty to reach the region where the lesions or traumas are located [4]. A safe and minimally invasive access to these areas would be a very important step in spine surgery.

This paper illustrates the design and fabrication of a first prototype of steerable endoscope for the navigation within the meningeal (or sub-arachnoid) space of the spinal cord. The main applications of such a device are: 1) to allow direct vision of the anatomy; 2) to perform some therapeutic treatment, like laser coagulation, local electrostimulation, local injection of drugs and cleaning procedure of arachnoidal fibrosis.

II. Description of the Working Environment

Our catheter is designed to navigate inside the spinal subarachnoid space in order to reach the target sites.

The boundaries and dimensions of this space vary widely along the length of the spinal cord, and the internal *CSF* possesses a variable dynamics. A schematic representation of the structure of the subarachnoid space is illustrated in fig.1.

The spinal cord is held in position by laterally oriented denticulate ligaments, 31 pairs of nerve roots (average diameter of 4 mm) and the filum terminale. The spinal canal can be approximated by 3 channels: the anterior, posterior and the lateral channels, in relation to the cord (see fig.2).

Generally, the ventral channel is narrower (1-3 mm) than the dorsal one (2-6 mm) [5]. The catheter should navigate through the 3 available channels. Studies on corps have demonstrated that a catheter with an external diameter of 2.2 mm can advance without causing any injury to the upper thoracic levels. While the dorsal and lateral channels allowed its passage in the thoracic region, a strong resistance was encountered at the ventral channel in the

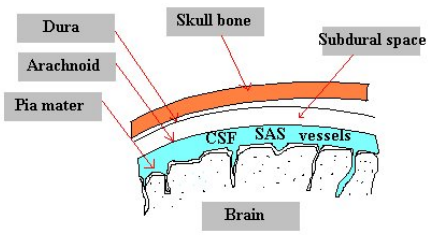

Fig. 1. Schematic representation of the spinal membranes.

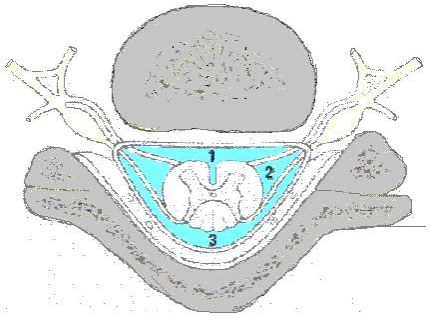

Fig. 2. The spinal subarachnoid space showing the boundaries and the channels (1-ventral, 2-lateral and 3-dorsal channel).

upper thoracic region [6]. Endoscopes of external diameter up to 1.5mm have visualized the entire spinal cord [7].

The cerebrospinal fluid in a human body ranges between 100 ml and 160 ml: 35 ml is in the brain, 25 ml around it, and 75 ml flowing in the spinal canal. Being secreted continuously at the rate of 0.35 ml/min, the total volume is replaced every 6-8 hours (about 3.7 times a day) [8]. The normal CSF pressure ranges from 4.5 to 13.5 mm of Hg (average 9.0 mm Hg) [9]. The fluid contains very few cells and proteins, its pH ranges from 7.31 to 7.35, its specific gravity is approximately 1.005 and the viscosity is 0.01 poise [10], resembling plasma; thus it can be replaced by an electrolytic solution, as long as the concentration, volume and pressure are maintained in the space. Such "Artificial CSF" is commercially available (ALZET osmotic pumps, DURECT Corp., Cupertino, CA).

CSF flow has features of both Poiseuille flow and pulsatile flow, and is primarily attributed to the pressure waves generated by pulsatile arterial blood flow and brain expansion. Along the spinal cord, the hydraulic diameter varies from 5 to 15 mm. Peak velocities are smaller than 7 cm/s; the mean maximum caudal velocity is around 2.91 cm/s corresponding to a mean maximum flow rate of 4.13 ml/s. The instantaneous Reynolds number at peak flow rate ranges from 170 to 450; the blunt velocity profile and the peaks located near the boundaries of the canal rather than at the midpoint between them show that inertial forces dominate over viscous forces [11], thus indicating a recirculant behaviour of the fluid.

The peak wall shear stress due to the CSF circulation in the spinal canal is typically less than 1.0 Pa with mean wall shear stress values close to zero [11]. The endoscope must be designed to minimize its contact with the walls, and in particular with the blood vessels on the pia membrane, which can be easily damaged. This objective can be achieved by the novel use of hydrojets.

III. The system

The above considerations indicate that the working field is very critical due to its small dimensions and to the presence of many delicate structures (blood vessels and nerve roots). Thus many constraints have to be considered in the development of the endoscopic system.

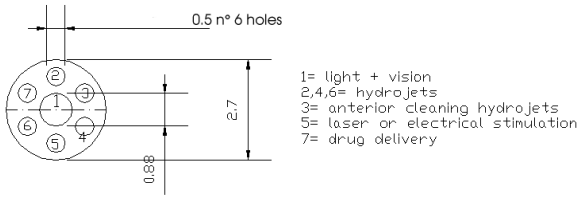

Fig. 3. Schematic representation of the catheter.

The overall system includes a catheter, a sustentation system, a steering system, a visualization system, and a set of instruments for local intervention on the spine.

A. The catheter

Several internal working channels are required, to allow vision, cleaning and drug delivery capabilities to the system. According to the anatomical constraints of the subarachnoid space and to the needed features of the catheter, the total diameter of the catheter must be less than 3 mm.

We use a commercially available co-extruded Polyimide catheter; it has an external diameter of 2.7 mm, and 7 internal lumen. The inner structure of the catheter is reported in fig.3.

Lumen no.2, 4, 6 were closed at the tip; holes whose diameter is 0.3 mm were produced in radial direction, 5 mm from the tip, by means of a miniature end-mill.

The central lumen is dedicated to the endoscope: the endoscope used in the system has an external diameter of 0.6 mm and a resolution of 3000 pixels, kindly provided by KARL STORZ GmbH & Co., Tuttlingen, Germany.

B. The sustentation system

In order not to touch the delicate structures of the subarachnoid space with the tip of the catheter, a hydraulic sustentation system has been developed. From the holes in the lumen no. 2, 4 and 6, a liquid similar to CSF is ejected radially with respect to the catheter.

Contacts between vessels or nerve roots and the catheter body are much less dangerous, according to medical experts. For this reason, hydrojets have been put only on the tip in the preliminary version of the device.

A precise control of the shape and the speed of the jets is essential in order not to damage the tissues.

C. The steering system

The same hydrojets system used for sustentation allows also the bending of the tip of the catheter, by varying the flow exiting from the hydrojets.

Literature reports many different ways for actuating the tip of a catheter ([12], [13], [14], [15]): in this paper a new

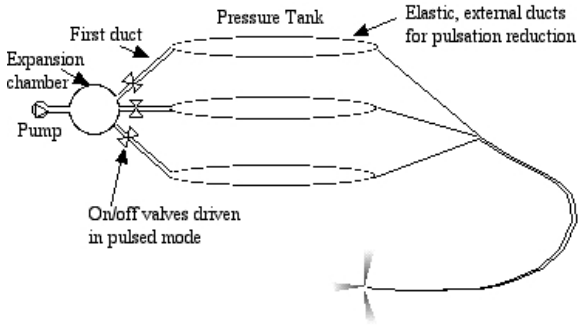

Fig. 4. Sketch of the system.

solution based on hydrodynamic sustentation is presented, whose essential features are high spatial resolution and stability.

D. The damping system

The architecture of the device is shown in fig.4.

Instead of using three different pumps, an architecture with one pump (regulating the pressure of an expansion chamber) and three valves, one for each duct, has been adopted. This solution was selected for two main reasons: pumps reaching the needed values of flow are extremely expensive. Moreover, the pressure inside the thecal sac has to be kept approximately constant (see section II): this is easier to be obtained if the source of pressurized liquid is only one, instead of three. In this way a safety condition can be directly implemented: the flow injected inside the subarachnoid space can be easily kept constant over time.

Proportional valves with the needed features in terms of flow rate, pressure range and linearity are not on the market; thus on-off valves (SIRAI V165) were used.

The basic idea is to produce three independent jets by means of ON-OFF valves driven in Pulse Width Modulation (PWM) mode. More precisely, referring to fig.5, each valve exits in a first tract of duct characterized by hydraulic resistance R_1, followed by a pressure tank whose compliance is C (volume increase / pressure); then a second duct follows, in the catheter itself, with resistance R_C.

In this way, high duty cycles are expected to inflate the elastic tank more than low ones. Different levels of pressure (p) can be obtained, energizing the catheter ducts while having the same input pressure in the system (p_i). The equations modeling this architecture are the following:

$$p = C \cdot V \tag{1}$$

$$V = \int_0^t (F_1 - F_C)dt \tag{2}$$

$$\begin{cases} F_1 = \dfrac{p_i - p}{R_1} & \text{on} \\ F_1 = 0 & \text{off} \end{cases} \tag{3}$$

$$F_C = \frac{p}{R_C} \tag{4}$$

Equation (1) is the relation between volume expansion of an elastic chamber (V) and internal pressure (p). Assuming the compliance C constant, it is correct to consider low deformations of the tank (less than 10%), in order to restrict operation to linear domain for the elastic tank. Equation (2) is the flow balance: F_1 is the flow from the first tract; F_C is the flow inside the second tract. Equations (3) and (4) express the hydraulic resistance of the ducts, constant because the flow is laminar (maximum Reynolds numbers in the ducts are in the order of 500).

A discrete parameters model can be acceptable if the ducts are much rigid and resistive with respect to the tank; this condition is easily achievable with appropriate tubing. From the expressions above, tank pressure can be derived:

$$\begin{cases} p = \left(p_0 - \dfrac{R_C}{R_1 + R_C} p_i\right) e^{-\frac{R_1+R_C}{C \cdot R_1 R_C} t} + \\ \quad + \dfrac{R_C}{R_1 + R_C} p_i & \text{on} \\ p = p_0 e^{-\frac{1}{C}\frac{R_1+R_C}{R_1 R_C} t} & \text{off} \end{cases} \tag{5}$$

where p_0 is the initial condition for tank pressure while switching valve state. Thanks to this result the whole behavior of the flows inside the catheter ducts is predicted, and it has been numerically simulated in a *Matlab* environment. In particular three parameters have been optimized: low pressure ripple, for avoiding any vibration during catheter operation; bandwidth, in order to have fast response and real time behavior of the system; dynamics, to obtain high differences in pressure between the situations in which a square wave signal having high rether than low duty cycle drives the valve. Such optimization can be pursued by acting on four parameters: PWM period T_v and duty cycle DC, hydraulic compliance C, and hydraulic resistance R_1.

E. Matlab Simulation

Equation (5) was numerically solved by using *Matlab* software. It was also analytically investigated in order to find the expression of the ripple R with T_v and DC as parameters, thus obtaining (6):

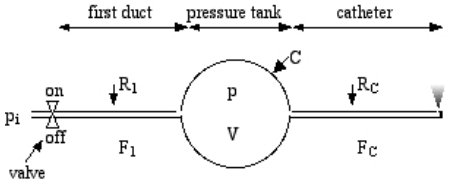

Fig. 5. Discrete parameters model of the PWM hydraulic circuit.

$$R(T_v, DC) = 1 - e^{-\frac{1}{CR_C} T_v (1-DC)} \quad (6)$$

Fig. 6 reports the simulation result for a system having 1 m long catheter ducts of 0.5 mm in diameter, and 0.3 m long resistive ducts R_1 with diameter equal to 0.5 mm. Pressure tank consists of a 60 cm long, 2.4 mm diameter duct having a 0.7 mm thick wall (see fig. 5 as reference); it is made out of Tygon© R-3603 polymer.

IV. Control System Description

The decision of using only one pump imposes the introduction of an "expansion chamber" between the pump and the valves, in order to keep the input pressure of the valves constant, also for different opening and closing times of the valves.

The main control loop of the system keeps the pressure inside the expansion chamber to a value set by the doctor.

The surgeon drives the duty cycles of the three valves by means of a joystick, thus causing the steering action of the tip.

The control board is completely digital. The programmable device used for the algorithm is a Microchip PIC16F877.

Fig.7 shows a representation of the system, from a control point of view.

A. The joystick

The surgeon drives the tip of the catheter by means of a joystick.

A calibration procedure has been implemented in order to allow the use of different types of joysticks, and to precisely compensate the gravity effect when the catheter is kept in horizontal position.

In order to avoid any adhesions or contacts, in no case a hydrojet can be turned completely off.

In order to implement the control of the tip by means of the joystick, a preliminary change of base is necessary:

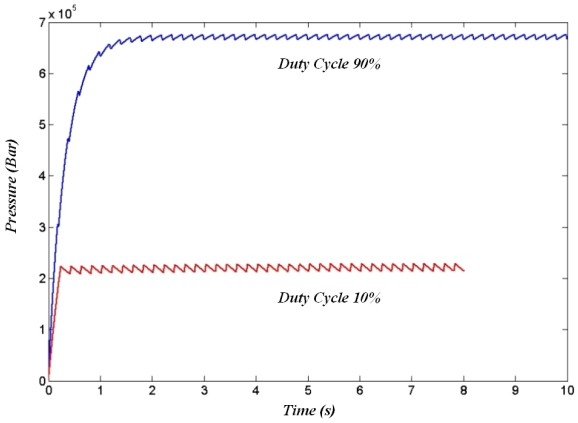

Fig. 6. Numerical simulation of the pressure ripple.

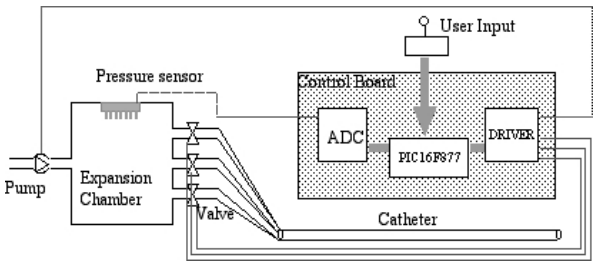

Fig. 7. Schematic representation of the control system.

starting from a $[S_x, S_y]$ position of the joystick, a combination $[F_A, F_B, F_C]$ of the three flows has to be computed (see fig.8).

The relation between the bases $[x,y]$ and $[A,B,C]$ is given by the following equations:

$$S_x = \frac{\sqrt{3}}{2}(F_C - F_B) \quad (7)$$

$$S_y = -A + \frac{1}{2}(F_B + F_C) \quad (8)$$

A third relation is necessary to make the system reversible. We decided to keep constant the total liquid flow injected into the subarachnoid space. This decision has been defined to make easier the control algorithm of the fluid extraction system: in fact, the pressure of the *CSF* inside the thecal sac must be kept constant. A too high pressure in the subarachnoid space has several drawbacks, from a simple postoperative headache, to macular haemorrhage and detachment of the retina ([1]). Thus a subsystem for evacuating excessive *CSF* has to be implemented.

This relation is

$$F_A + F_B + F_C = k \quad (9)$$

where k is constant.

If we define $D_x = S_x - S_{x_0}$, $D_y = S_y - S_{y_0}$ the displacements from a calibration position $[S_{x_0}, S_{y_0}]$, the formulas used to obtain F_A, F_B, F_C from D_x and D_y are:

$$F_A = k - \frac{2}{3} D_y \quad (10)$$

$$F_B = k - \frac{D_x}{\sqrt{3}} + \frac{D_y}{3} \quad (11)$$

$$F_C = k + \frac{D_x}{\sqrt{3}} + \frac{D_y}{3} \quad (12)$$

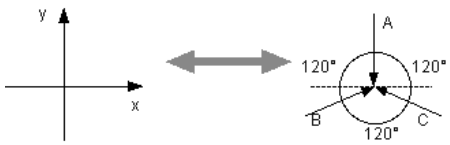

Fig. 8. Relation between $[x,y]$ and $[A,B,C]$ bases.

B. Valves

As explained in the previous section, one on-off valve is used for each channel. The strategy exploited to vary the flow through this kind of valves consists of driving them in PWM mode. The valve is turned on and off by a square wave of frequency f_v, whose duty cycle is proportional to the flow ϕ through the valve itself.

The choice of the frequency f_v is rather delicate. In fact this driving method produces a ripple R in the flow ϕ, whose amplitude increases with the period of the square wave T_v. Equation (6) relates the ripple R to the period T_v.

On the other hand, mechanical constraints of the valve impose a minimum switch on time t_{on-min} and a minimum switch off time $t_{off-min}$: thus, a minimum in the applicable T_v is $T_{v-min} = t_{on-min} + t_{off-min}$. In this case the duty cycle (DC) can have only a precise value:

$$DC_{min} = \frac{t_{on-min}}{t_{on-min} + t_{off-min}} \cdot 100 \tag{13}$$

For our valves, this value is 50%, being that $t_{on-min} = t_{off-min} = 5ms$: the modulation of the DC is impossible.

If we define *DC modulation factor* the ratio:

$$\begin{aligned} M(T_v) &= \frac{T_v - t_{on-min} - t_{off-min}}{T_v} \cdot 100 = \\ &= (1 - \frac{T_{v-min}}{T_v}) \cdot 100, \end{aligned} \tag{14}$$

the optimal situation, from the modulation capability point of view, would be to have a very low f_v.

The choice of f_v is a trade off between modulation and ripple requirements.

In fig.9 the plots of $M(T_v)$ and $R(T_v, D_{min})$, are reported: in fact, when $D = D_{min}$, the ripple has its highest value. In this case (6) becomes:

$$R(T_v) = 1 - e^{-\frac{T_v - T_{v-min}}{C \cdot R_C}} \tag{15}$$

From the plot, in order to keep ripple lower than 15% for every value of D and *modulation factor* greater than 85%, the optimal range of f_v goes from 6 Hz to 14 Hz.

In any case the frequency f_v can be set at any value, from 3.8 Hz up to 70 Hz, to allow the use of different types of valves.

V. Tests

The performances of the sustentation and steering system were tested by using a specifically conceived test set-up (see fig.10), consisting of a transparent tank filled with water. The top of the tank has several insertion channels at different angles, to simulate different situations in approaching the spinal canal.

By actuating only one hydrojet of a 30 cm long immersed catheter portion, an input liquid pressure of 4 bar produced a lateral tip displacement of 1 cm (see fig.11). Setting the pressure to 6.6 bar, a displacement of 3 cm was measured.

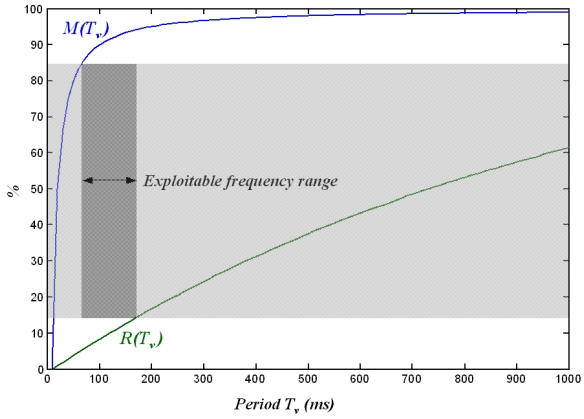

Fig. 9. Plots of $M(T_v)$ and $R(T_v, P)$.

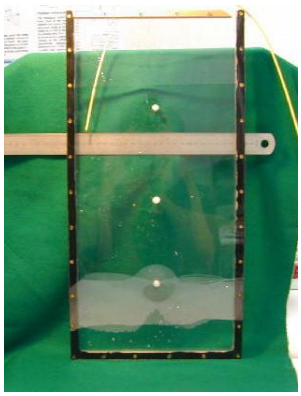

Fig. 10. Test set-up used for the 1-hydrojet catheter.

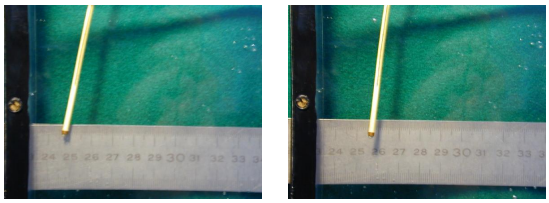

(a) Equilibrium condition. Input pressure=0bar.

(b) Condition with input pressure=4bar.

Fig. 11. Quantitative test of the bending performances of the 1-hydrojet catheter, under an input pressure of 4 bar.

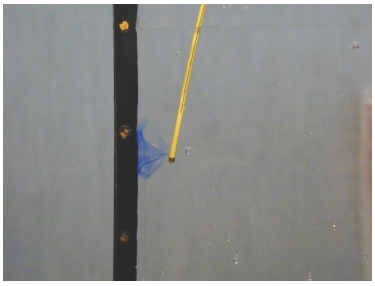

Fig. 12. Qualitative visualization of a hydrojet approaching a wall.

The 3 hydrojets catheter has been tested in a larger tank filled with water, on an artificial path. With a pressure in the expansion chamber of 6.6 bar, a lateral displacement of 2.5 cm from the central equilibrium position was achieved.

VI. Conclusions and future work

We proposed a new catheter system for spinal subarachnoid endoscopy, optimized for safe navigation in liquid environments. A novel use of hydraulic control has been presented. The catheter proposed is a fine active bending catheter using three lateral hydrojets at the tip, driven by means of a joystick.

The bending performance of the proposed catheter is largely sufficient for avoiding the collisions with the most delicate structures in the subarachnoid space.

In fig.12 the shape of the hydrojet near the tank wall is visible. A deep study of the interactions of the hydrojet with the *arachnoid* and *pia mater* is necessary, in order to maximize the steering action while minimizing the pressure on these structures. The shape of the hydrojet will be optimized by using appropriate microfluidic simulations (CoventorWare).

A model of the spine is being developed including the structures in the subarachnoid space: nerve roots, blood vessels, pulsating liquid, walls, fibrous tissue [7]; the physical properties of these structures must be as close as possible to the real ones.

A quantitative set of in-vitro tests has to be performed by using the new model of the spine. The steering capabilities of the catheter have to be tested in more complex paths. Finally, a set of ex-vivo and in-vivo experiments are being planned.

VII. Acknowledgements

This work is being carried out under the ”Quality of Life and Management of Living Resources” project Mi.N.O.S.C. (MicroNeuroendoscopy of Spinal Cord - N. QLG5-CT-2001-02150)

VIII. References

[1] L. Saberski and P. Dickey, “Spinal canal endoscopy,” *Min Invas Ther & Allied Technol 1998:7/2*, pp. 119–122, 1998.

[2] D. Chatenever, “Minimally invasive surgical visualization- past, present, and future,” *J. Minim. Invasive Spinal Tech.*, 2001.

[3] J. Warnke, M. Tschabitscher, and A. Nobles, “Thecaloscopy: the endoscopy of the lumbar subarachnoid space, part 1: Historical review and own cadaver studies,” *Minim. Invas. Neurosurgery*, pp. 61–64, 2001 (44).

[4] T. Eguchi, N. Tamaki, and H. Kurata, “Endoscopy of the spinal cord: cadaveric study and clinical experience,” *Minim. Invas. Neurosurgery*, pp. 146–151, 1999 (42).

[5] K. Malinowsky, “Massbestimmungen am wirbelkanal: Dage der einzelnen teile und sonstige verŁltnisse desselben,” *Arch. F. Anat. Physiol. U. Wissenschaftl Med*, vol. 8, p. 249, 1910.

[6] S. Shimada and Tamaki, “Assessment of safety and feasibility of spinal endoscope in the thoracic and lumbar region: A cadaveric study,” *Kobe J. Med. Sci.*, vol. 47, pp. 263–272, December 2001.

[7] S. Uchiyama, K. Hasegawa, and T. Homma, “Ultrafine flexible spinal endoscope (myeloscope) and discovery of an unreported subarachnoid lesion,” *SPINE*, vol. 23, no. 21, pp. 2358–2362, 1998.

[8] *Ganong’s Review of Medical Physiology*. 17 ed.

[9] D. Greitz, R. Wirestam, A. Franck, B. Nordell, C. Thomsen, and F. Stahlberg, “Pulsatile brain movement and associated hydrodynamics studied by magnetic resonance phase imaging. The Monro-Kellie doctrine revisited.,” *Neuroradiology*, vol. 34(5), pp. 370–380, 1992.

[10] Bloomfield, I. G. Johnston, I. H., Bilston, and L. E., “Effects of proteins, blood cells and glucose on the viscosity of cerebrospinal fluid,” *Pediatr. Neurosurg.*, vol. 28, p. 246251, 1998.

[11] F. Loth, M. Yardimci, and N. Alperin, “Hydrodynamic modeling of cerebrospinal fluid motion within the spinal cavity,” *Journal of Biomechanical Engineering*, vol. 123(1), pp. 71–79, February 2001.

[12] H. Adachi, H. Takizawa, R. Ohta, and H. Tosaka, “Development of a microfine active bending catheter equipped with MIF contact sensors,” *Proceedings of the sixth international micromachine symposium*, pp. 193–198, November 9-10, 2000.

[13] K.-T. Park and M. Esashi, “A multilink active catheter with polyimide-based integrated CMos interface circuits,” *Journal of microelectromechanical systems*, vol. 8, December 1999.

[14] K. Ikuta, H. Ichikawa, and K. Suzuki, “Safety-active catheter with multiple-segments driven by micro hydraulic actuators,”

[15] Y.Haga, Y. Tanahashi, and M. Esashi, “Small diameter active catheter using shape memory alloy,” *0-7803-4412-X/98 IEEE*, 1998.